RSC Advances

PAPER

Cite this: *RSC Adv.*, 2024, **14**, 30180

Nano silver oxide-modified activated carbon as a novel catalyst for efficient removal of bacteria and micropollutants in aquatic environment†

Jianping Deng,[ab] Yong Liu,[ab] Shuanglin Gui,[ab] Qizhen Yi[ab] and Hanbing Nie *[ab]

Received 24th June 2024
Accepted 17th August 2024

DOI: 10.1039/d4ra04604h

rsc.li/rsc-advances

Heterogeneous Fenton process is a promising water treatment technology for sterilization and degradation of organic pollutants, due to the strong oxidation of hydroxyl radicals ($OH^•$) generated. However, the low H_2O_2 activation efficiency and the instability of catalyst leading to low $OH^•$ production restricted development of this technology. Herein, we synthesized a novel porous activated carbon-loaded nano silver oxide (nAg_2O/AC) catalyst to enhance the activation of H_2O_2 for removing bacteria (*E. coli*) and micropollutants (Tetracycline, TC) from water. In the nAg_2O/AC Fenton system, reductive hydroxyl groups on AC accelerated Ag(I)/Ag cycle through mediated electron transfer, which markedly increased H_2O_2 activation efficiency to 73.7% (About 2.9 times that of traditional Fenton). Hence, nAg_2O/AC Fenton achieved up to 6.0 log and 100% removal efficiency for *E. coli* and TC, respectively. The $OH^•$ as the major oxidizing species in nAg_2O/AC Fenton system was detected and verified by radical scavenging tests and electron spin resonance (ESR) measurement. After 4 and 5 cycles of experiments, the removal of *E. coli* and TC still reached 5.2 log and 96%, respectively, confirming good stability of nAg_2O/AC for considerable application prospects. This study concluded that nAg_2O/AC is a promising H_2O_2 catalyst for simultaneous removal of bacteria and micropollutants in aqueous environment.

1 Introduction

Water environment security is closely related to social development and human health. With the advancement of technology and the widespread use of antibiotics, antibiotic resistant bacteria and trace pollutants have been frequently detected in various water bodies,[1] posing a serious threat to aquatic ecology and human health. Traditional chlorination method for treating such bacteria is becoming increasingly inadequate,[2] and even worse, it could react with micropollutants to generate toxic byproducts (*e.g.*, halogenated organic compounds and chlorate) resulting in secondary contamination.[3] Instead, various emerging technologies including membrane filtration,[4,5] chemical reduction/oxidation,[6–8] electrochemistry[9] and photocatalytic degradation[10–13] have been studied for removing bacteria and micropollutants. Despite some progress in experiments, the practical application of these technologies is still constrained by high energy consumption, low efficiency, and complex operating conditions.

Advanced oxidation processes (AOPs) are recognized as a promising water purification technology,[14] owing to the high-efficiency sterilization and degradation effect of strong oxidizing reactive oxygen species (ROS) (*e.g.*, $OH^•$ and $O_2^{•-}$) produced. [15] It is well known that Fenton reaction is one of the most efficient method in AOPs, which can produce abundant $OH^•$ through Fe^{2+}/H_2O_2 reaction. [16] Nevertheless, there are still some defects in Fenton reaction such as the low activation efficiency of H_2O_2, restriction of pH application range (2.0–4.0) and massive ferric salt precipitation as solid waste.[17] Given this, heterogeneous Fenton catalysts are developed and applied,[18] especially various nanometal oxides with natural antibacterial property and potential catalytic activity.[19]

Nano silver oxide (nAg_2O) has better sterilization and catalytic performance compared to other metal oxides, such as Fe_2O_3, Co_2O_3, CuO and MoO_2.[20] However, when nAg_2O is used alone, its activity is still low and is greatly affected by agglomeration.[21] Activated carbon (AC) is a satisfactory alternative carrier for nanoparticles due to its excellent conductivity and large surface area. Our previous work showed that loading nAg_2O onto AC can effectively improve its dispersibility and reactivity, and achieve effective sterilization by activating dissolved oxygen to generate superoxide radical at a wide pH range.[22] This means that nAg_2O/AC, if used as a heterogeneous catalyst, would have enormous potential to activate hydrogen peroxide (H_2O_2). As a common green oxidant in water treatment, H_2O_2 is more easily activated to produce stronger oxidizing hydroxyl radicals ($OH^•$) which possess better sterilization and organic matter degradation effects.[23] In addition, due to its stability and activity over a wide pH range,

[a]Institute of Energy Research, Jiangxi Academy of Sciences, Nanchang, 330096, China. E-mail: niehanbing221@126.com

[b]Jiangxi Carbon Neutralization Research Center, Nanchang, 330096, China

† Electronic supplementary information (ESI) available. See DOI: https://doi.org/10.1039/d4ra04604h

nAg_2O/AC as a heterogeneous catalyst is expected to improve the decomposition efficiency of H_2O_2 producing more $OH^•$, ultimately achieving efficient removal of bacteria and organic micropollutants in water.

In this work, nAg_2O/AC as a novel heterogeneous Fenton catalyst is developed to enhance H_2O_2 activation efficiency for more $OH^•$ radicals' production to remove bacteria and micropollutants in water. The nAg_2O/AC catalyst was synthesized by a simple hydrothermal method and applied for H_2O_2 activation to treat wastewater. *Escherichia coli* (*E. coli*) and tetracycline (TC) were regarded as the target bacteria and micropollutants, respectively. A series of characterization techniques were used to investigate surface characteristics of catalysts and further explore electron transfer process between nAg_2O and AC. The effects of initial pH in Fenton process were investigated in the range of pH 5.0–9.0. Subsequently, cycle and regeneration tests were carried out for estimating the useful life of nAg_2O/AC during treatment. Mechanism of nAg_2O/AC Fenton process was explored through quenching experiments and ESR measurement. In addition, the decomposition rate of H_2O_2 was further quantitatively analyzed by fluorescence spectroscopy. Consequently, the obtained findings could be useful in providing significant insight into the development of novel heterogeneous Fenton catalysts and their application in the treatment of composite pollutants in water.

2 Materials and methods

2.1 Materials and chemicals

Details of chemicals and materials are provided in Text S1 of the ESI.†

2.2 Preparation of catalysts

Based on our previous studies of modifying activated carbon with metal oxides,[24] a facile impregnation-calcination method was applied to prepare the nAg_2O/AC catalyst. Briefly, 316 mg $AgNO_3$ and 200 mg PVP was mixed evenly in 200 mL deionized water. Subsequently, 20.0 g activated carbon was poured into and mixed evenly. After 12 h of magnetic stirring, the beaker was allowed to stand for 24 h. After being filtered and washed to neutral with pure water, the remaining solid was placed at 75 °C for 12 h to obtain nAg_2O/AC catalyst.

To measure the silver-loading rate, the nAg_2O/AC was treated with nitric acid for 8 h to elute silver and the silver concentration was measured by an atomic absorption spectrometer (AAS). The silver-loading rate was determined as ±1.5%. Unsupported nAg_2O was synthesized as a control. Briefly, under magnetic stirring, 1.0 g of $AgNO_3$ was dissolved in 100 mL deionized water in a conical flask. The pH value was adjusted to 12 by 1 M NaOH. The nAg_2O was achieved by filtering and drying the residue at 70 °C for 24 h.

2.3 Experiments

Batch experiments were performed in 200 mL conical flasks. Each flask contained 100 mL bacteria (10^6 CFU mL^{-1} *E. coli*) and micropollutants (1 mg L^{-1} TC), in which the preparation of *E. coli* solutions is detailed in Text S2.† After injecting 0.1 g nAg_2O/AC and 3.2 mM H_2O_2, the flask was sealed with parafilm and shaken at 30 °C to start nAg_2O/AC-H_2O_2 heterogeneous Fenton reaction for removing bacteria and micropollutants. As the reaction lasted for 1, 3, 5, 10 and 15 min respectively, 1 mL solution was collected to detect TC concentration. Meanwhile, 0.1 mL solution was taken out to calculate bacterial concentration by plate counting method. The residual *E. coli* density was calculated by the number of colonies and utilized to evaluate the inactivation efficiency [25] and the detailed identification process is described in Text S2.† Similarly, as control experiments, the nAg_2O/H_2O_2, AC/H_2O_2, nAg_2O/AC alone and H_2O_2 alone systems were also carried out according to the above procedures, respectively. After reaction, silver ions (Ag^+) in water were detected.

Cycle and regeneration tests were conducted to evaluate stability and reusability of the catalysts.[26] The first cycle reaction of nAg_2O/AC catalyst was similar to the heterogeneous Fenton process described above. During reaction, removal efficiency and leached Ag^+ were measured. The first experiment ended and the nAg_2O/AC catalyst was recovered through filtration and drying. Immediately, recycled nAg_2O/AC was applied for 5 cyclic tests as described in the first process. After cycle tests, using nitric acid to remove silver on activated carbon, and regained activated carbon was used for synthesizing catalysts based on the previous synthesis method. The regenerated nAg_2O/AC was then used in heterogeneous Fenton process for removing pollutants to evaluate reusability.

2.4 Effects of scavengers and detection of $OH^•$

The methods of detection in this study are shown in Text S3 of the ESI.†

2.5 Analytical methods

Scanning electron microscope (SEM, Hitachi S-4500, Japan) was used to characterize microstructure of nAg_2O/AC catalyst before and after reaction. The crystal phase on catalyst surface was determined by X-ray diffraction (XRD, D8 ADVANCE, Bruker, Germany) with the Cu-Kα radiation source. Besides, An X-ray photoelectron spectroscopy (XPS, K-Alpha, USA) with a Ka-Al radiation was applied to analyze the valence change of different elements in nAg_2O/AC. To verify free radicals produced in these Fenton systems, electron spin resonance spectrometer (ESR, Bruker EMX A300-10/12, Germany) was applied with 5, 5-dimethyl-1-pyrroline-*N*-oxide (DMPO) as spin-trapping agents.[27] Flame atomic absorption spectrophotometer (FAAS, HITACHI Z-2000, Japan) was utilized to identify the concentration of Ag^+ in solution.

The residual *E. coli* density (log CFU mL^{-1}) was calculated according to eqn (1).

$$E.\ coli\ \text{density} = \log_{10}C \quad (1)$$

where C is the bacterial density at t min.

The Ag leaching rate in nAg_2O/AC was counted using eqn (2).

$$\text{Leaching rate} = (\text{leached Ag})/(\text{loaded Ag}) \times 100\% \quad (2)$$

3 Results and discussion

3.1 Characterization of catalysts

A comprehensive study was conducted on the physicochemical properties and changes of nAg_2O/AC catalysts before and after reaction in the nAg_2O/AC-H_2O_2 system, providing basic support for revealing the reaction mechanism of nAg_2O/AC activating H_2O_2.

X-ray diffraction analysis (Fig. 1a) was performed on nAg_2O/AC. The nAg_2O/AC diffraction peaks at 26.8°, 32.7°, 38.2°, 55.3°, 65.5° before reaction corresponded to (110), (111), (200), (220), and (311) crystal planes of the Ag_2O standard diffraction card (JCPDF card no.75-1532), [28] respectively. After the reaction, these diffraction peaks showed certain enhancement, weakening, or disappearance. For example, the peak at 38.1° weakened, while the peak at 65.6° disappeared. This phenomenon may be caused by the reduction of catalyst particles or phase transformation during the reaction process. In addition, the characteristic diffraction peaks of AC at 25° and 44° showed some enhancement after the reaction, indicating that the carbon matrix of the catalyst was partially exposed after reaction.

Composition and changes of nAg_2O/AC functional groups before and after the reaction were analyzed by FTIR, as shown in Fig. 1b. Stretching vibration characteristic peaks of O–H, C–H, C═O, C═C, C–C and C–O appeared respectively at frequency bands 3420, 2817, 1735, 1519, 1360 and 938 cm^{-1} of nAg_2O/AC before reaction.[29] In addition, characteristic absorption peaks at 502 and 613 cm^{-1} corresponded to the stretching vibration of Ag–O.[30] Compared with that before reaction, many vibration peaks of nAg_2O/AC appeared to be strengthened, weakened, disappeared, or shifted after the reaction. For example, the C═O vibration peak at 1735 cm^{-1} and C–C vibration peak at 1360 cm^{-1} increased, the O–H vibration peak at 3420 cm^{-1} decreased, and the C–H vibration peak at 2817 cm^{-1} and Ag–O vibration peak at 502 and 613 cm^{-1} shifted. These phenomena indicated that nAg_2O existed in the modified AC, and the functional group type of AC surface had changed significantly during reaction, which meant that there may be a strong redox reaction between nAg_2O/AC and H_2O_2.

Surface structures and composition of nAg_2O/AC during heterogeneous Fenton progress were measured as Fig. 2 presented. The surface of fresh AC had abundant and irregular pores, which was conducive to its modification by nAg_2O particles. After AC was modified, some nano-sized aggregates were evenly distributed on its surfaces and pores and these aggregates were probably ascribed to nAg_2O. According to EDS analysis in Table S1,† nAg_2O/AC contained 1.5% Ag compared to fresh AC, implying the successful loading of nAg_2O on AC surface. In addition, EDS mapping images also showed that silver was effectively and evenly loaded on AC. The above results were also in agreement with XRD and FTIR results. After Fenton reaction, there was little change in the microstructure of nAg_2O/AC and the silver content lost slightly by about 0.8%. These results indicated that the binding of nAg_2O/AC composite materials was relatively stable before and after the reaction, providing reliable theoretical data support for the subsequent cycling and stability of the catalyst.

As illustrated in Fig. 3, X-ray photoelectron spectra (XPS) was used for elemental analysis. Fig. 3a displayed minimal changes of Ag, O and C peaks before and after reaction. This suggested stability of catalyst, corresponding to previous XRD and SEM analysis. The Ag 3d XPS spectrum of nAg_2O/AC (Fig. 3b) exhibited two major peaks at 374.2 and 368.1 eV, respectively, which could be fitted with two components.[31] The diffraction peaks at 374.6 and 368.6 eV were attributed to Ag, whereas the peaks centered at 373.9 and 368.9 eV were assigned to Ag(I).[32] According to peak intensity, the content of Ag(I) and Ag in nAg_2O/AC before reaction was equivalent, but Ag(I) was significantly higher than Ag after the reaction. This phenomenon indicated that nAg_2O/AC occurred an oxidation–reduction reaction during the activation of H_2O_2, leading to the oxidation of Ag to Ag(I). Fig. 3c and d depict the high-resolution spectra of nAg_2O/AC before and after reaction, and the composition of each functional group is obtained through peak fitting. The peak intensity of each functional group showed different levels of enhancement or weakening. For example, the C–OH peak exhibited a significant decrease during reaction process, while the C–C and C–O peaks increased after the reaction. This may be attributed to the oxidation of reducing C–OH group during reaction, which may be accompanied by the reduction reaction of Ag(I) to Ag. This phenomenon was consistent with the formation of Ag in Fig. 3b and consistent with the changes in various functional groups in the previous FTIR analysis. Due to

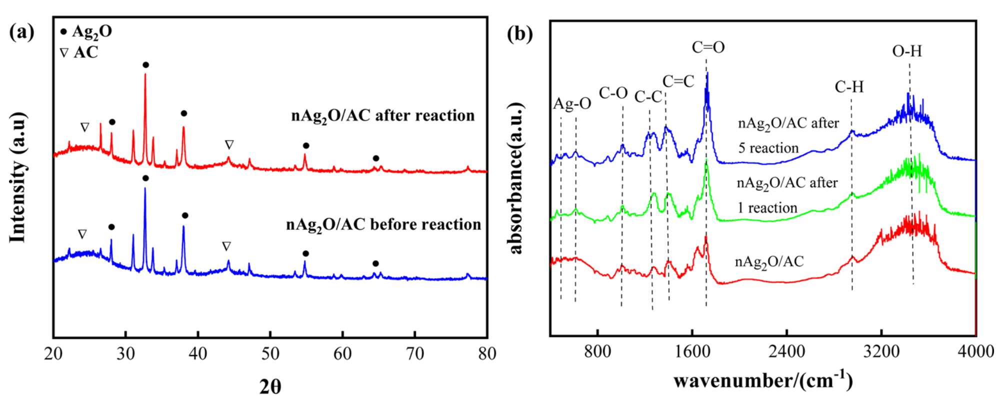

Fig. 1 (a) XRD patterns and (b) FTIR spectra of nAg_2O/AC in reaction.

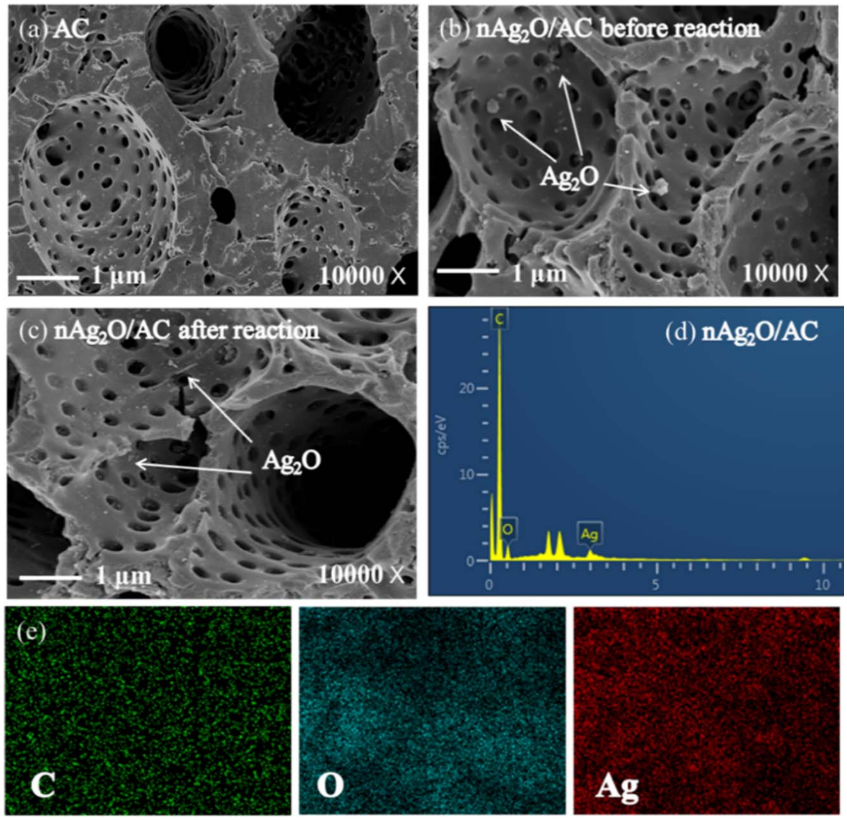

Fig. 2 (a–e) SEM-EDS patterns of nAg_2O/AC before and after reaction.

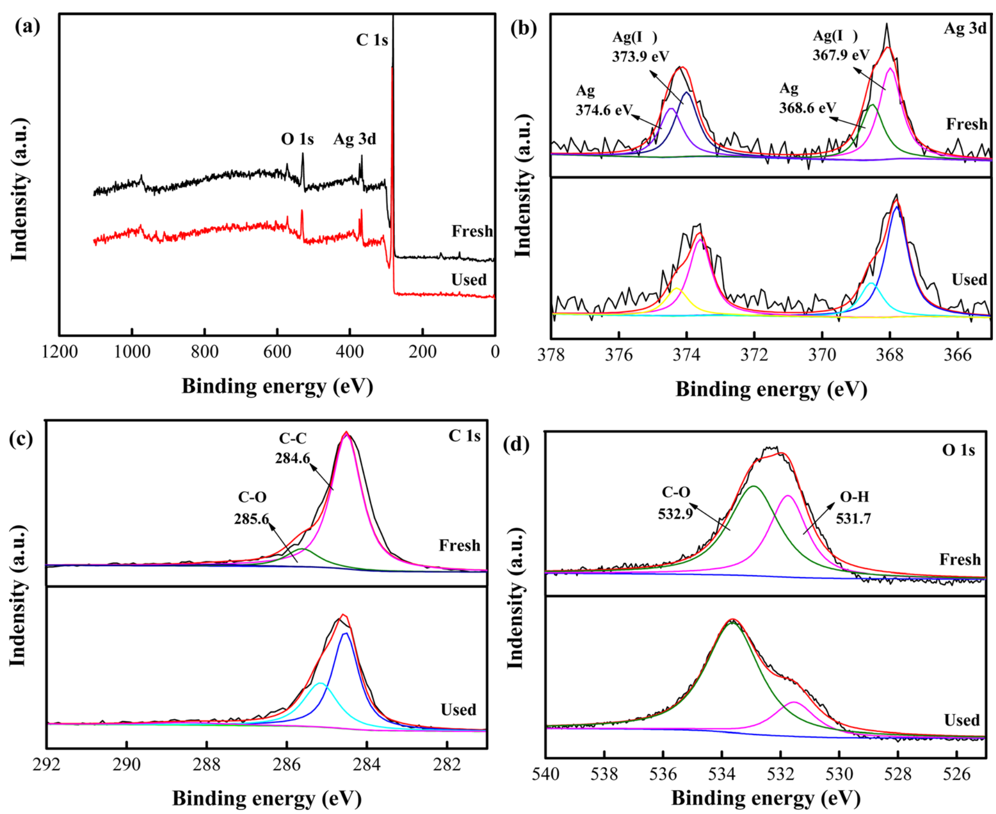

Fig. 3 XPS survey of (a) nAg_2O/AC, high-resolution XPS survey of (b) Ag 3d, (c) C 1s and (d) O 1s.

the ability of Ag to activate H_2O_2 to produce strong oxidizing $OH^{\bullet}$, the changes in functional groups and elemental states mentioned above are of great significance for the decontamination performance of $nAg_2O/AC\text{-}H_2O_2$ systems in water.

3.2 Removal performance

To investigate the enhanced removal performance of $nAg_2O/AC\text{-}H_2O_2$ heterogeneous Fenton system for *E. coli* and TC, it was compared with control systems such as nAg_2O/AC system, H_2O_2 system, $AC\text{-}H_2O_2$ system, and $nAg_2O\text{–}H_2O_2$ system, as illustrated in Fig. 4a and c. From the results, it can be seen that compared to the bacterial density under natural conditions (5.8 log), the H_2O_2 system, $AC\text{-}H_2O_2$ system, and $nAg_2O\text{–}H_2O_2$ system only reduced the bacterial density to 5.2, 5.1, and 4.6 log after 15 min of reaction, indicating that the oxidative sterilization ability of H_2O_2 was weak, and AC had almost no activation effect on H_2O_2, while nAg_2O had very limited activation ability on H_2O_2. Although the nAg_2O/AC system exhibited a slightly stronger sterilization effect, it only dropped to 4.1 log within 15 min. As mentioned in the previous work, it took a long time (about 3 hours) for nAg_2O/AC to achieve good sterilization effect, making it difficult to achieve satisfactory sterilization effect in a short period of time. However, once nAg_2O/AC and H_2O_2 participated in reaction together, cell density decreased rapidly and was close to 0 log at 10 min. The high inactivation efficiency displayed in nAg_2O/AC Fenton system also confirmed the excellent catalytic performance of nAg_2O/AC for H_2O_2. Similar removal results (Fig. 4c) can be obtained in the treatment of TC micropollutants. Compared with the control systems, the nAg_2O/AC Fenton system rapidly and completely degraded TC micropollutants within five minutes, indicating that the nAg_2O/AC Fenton system had excellent removal performance for both bacteria and organic micropollutants, which is of great significance for the treatment of multiplex pollutants in actual wastewater.

Dose of H_2O_2 exhibited a significant impact on sterilization efficiency as illustrated in Fig. 4b and d. Within a certain range, as the dosage of H_2O_2 increased, the sterilization efficiency also increased. However, increasing the dosage beyond a certain concentration led to a decrease in sterilization efficiency. When the dosage of H_2O_2 was 1, 2, and 4 mM, respectively, the bacterial survival density of the corresponding system decreased to 2.9, 1.2, and 0 log after 15 min of reaction, indicating that increasing the dosage of H_2O_2 within this range would bring more reactive oxygen species, thereby significantly improving sterilization efficiency. However, when the dosage of H_2O_2 further increased to 8 mM, the sterilization rate and efficiency of the system decreased significantly, indicating that H_2O_2 was already in excess and could undergo scavenging reactions with reactive oxygen species (see eqn (3) and (4)),[33] resulting in a decrease in the effective free radicals available for

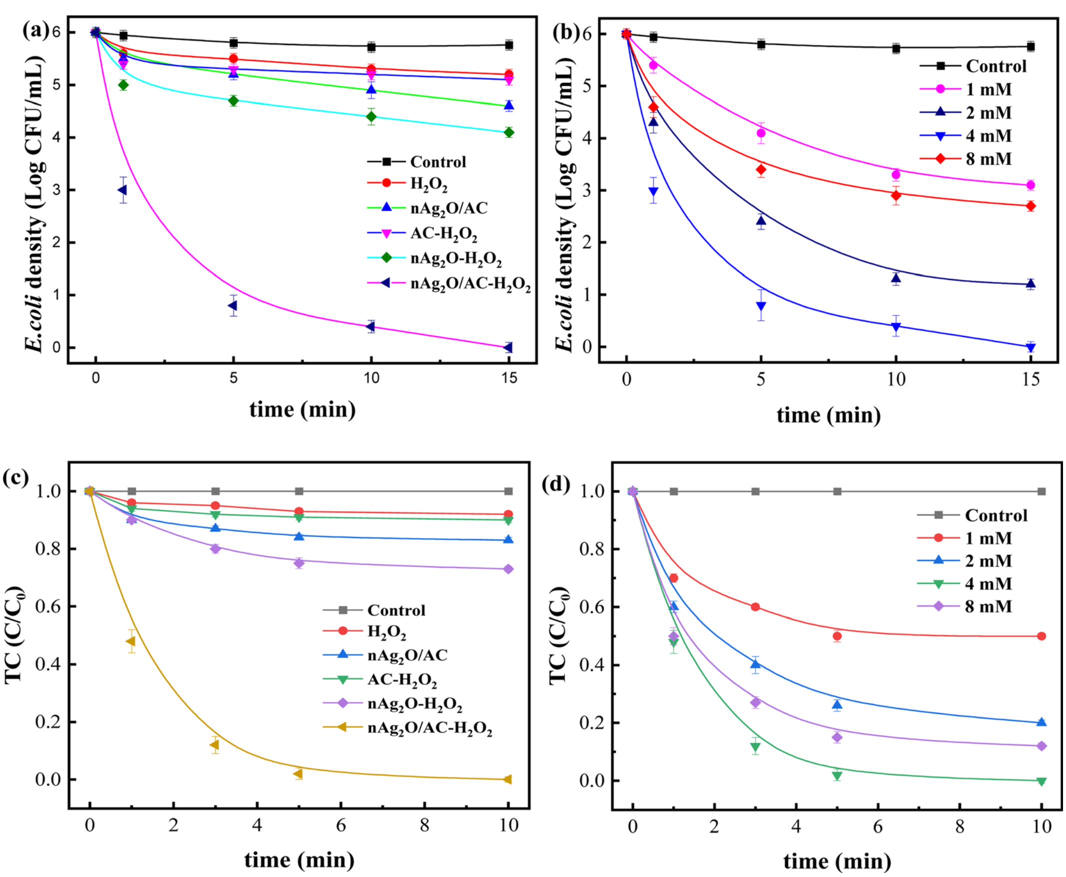

Fig. 4 Removal of (a) *E. coli* and (c) TC in different reaction systems; effect of H_2O_2 dosage on the removal of (b) *E. coli* and (d) TC in nAg_2O/AC Fenton system. Reaction conditions: 1 g L^{-1} nAg_2O/AC dosage, 4 mM H_2O_2, 10^6 CFU mL^{-1} *E. coli*, 1 mg L^{-1} TC, initial pH 7.0.

attacking bacteria. At the same time, effect of H_2O_2 dosage on TC removal exhibited a consistent trend, so an appropriate oxidant dosage was crucial for reaction efficiency. In addition, increasing the amount of H_2O_2 used would also result in higher reagent costs. Considering efficiency and cost, the appropriate dosage of 4 mM H_2O_2 is recommended.

$$H_2O_2 + OH^{\cdot} \rightarrow HO_2^{\cdot} + H_2O \quad (3)$$

$$HO_2^{\cdot} + OH^{\cdot} \rightarrow O_2 + H_2O \quad (4)$$

The nAg_2O/AC catalyst is also competitive compared with the previously reported Fenton-like catalyst, both in terms of removal efficiency and rate (Tables S2–S4†). These comparisons suggested the great potential of nAg_2O/AC in activating H_2O_2 for simultaneous removal of bacteria and micropollutions.

The composition of real water environment is very complex, and various anions and cations contained inside may have important impact on nAg_2O/AC Fenton reaction process. Therefore, the influence of common ions (cations such as K^+, Na^+, Ca^{2+}, Mg^{2+}, and anions such as Cl^-, SO_4^{2-}, NO_3^-, HCO_3^-) in water on the system was investigated as shown in Fig. 5.

Fig. 5a and b showed that cations in water generally had a slight impact on removal efficiency, with K^+ and Na^+ having almost no effect on sterilization process of the system, while Ca^{2+} and Mg^{2+} had only a small impact, possibly due to their

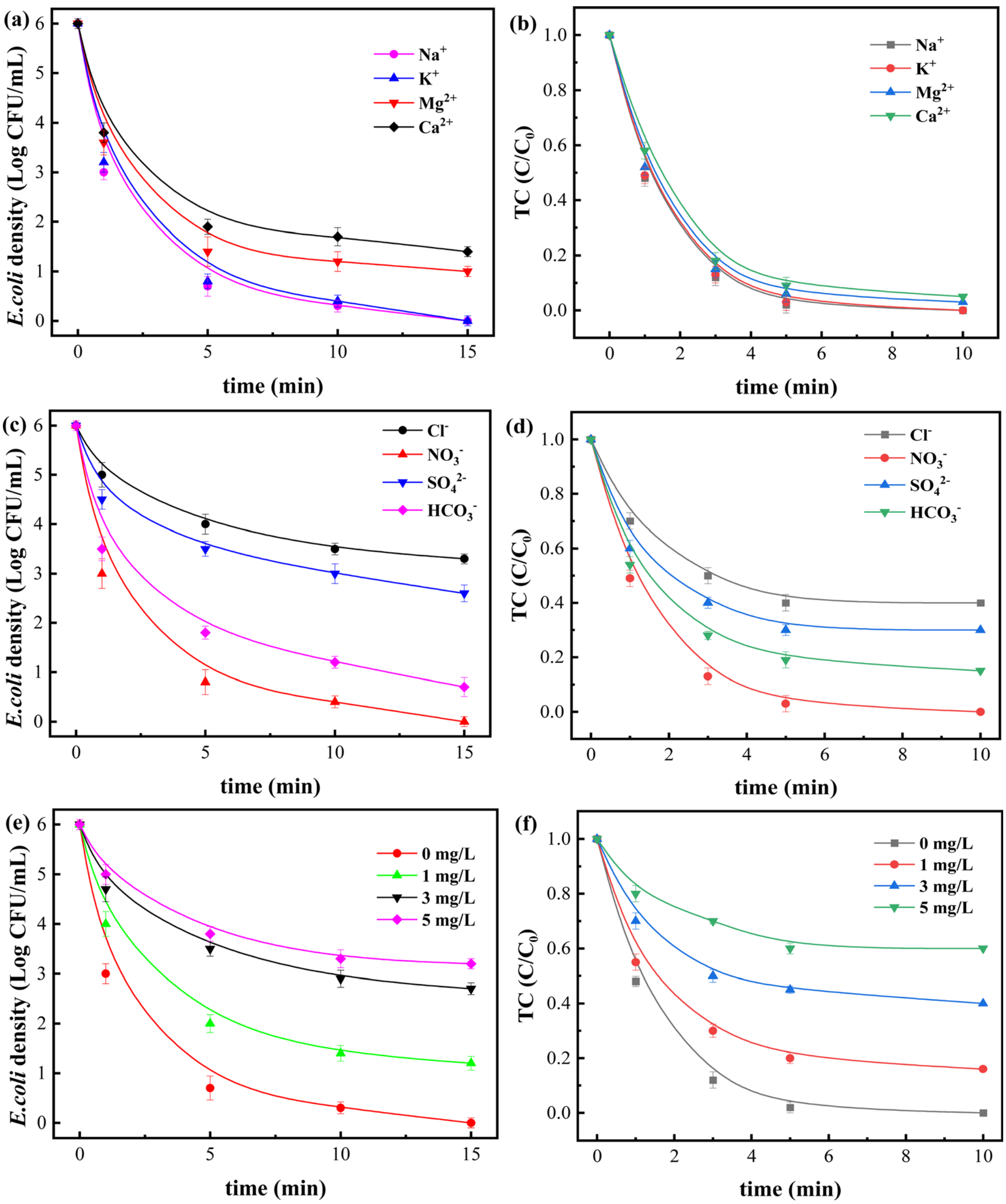

Fig. 5 Effect of coexisting ions (a and b) cations and (c and d) anions and (e and f) NOM in nAg_2O/AC Fenton system. Reaction conditions: 1 g L^{-1} nAg_2O/AC dosage, 4 mM H_2O_2, 10^6 CFU mL^{-1} *E. coli*, 1 mg L^{-1} TC, initial pH 7.0, temperature 30 °C.

participation in the competition of catalyst surface sites or their susceptibility to hydrolysis disrupting acid–base balance. [34] In contrast, anions had a more significant impact on the reaction process. As shown in Fig. 5c and d, when Cl^- and SO_4^{2-} coexisted in the nAg_2O/AC Fenton system, the bacterial survival density significantly increased from 0 to 3.2 and 2.6 log CFU mL^{-1}, respectively, and the residual ratio of TC also increased from 0 to 0.42 and 0.31. This phenomenon may be attributed to the easier complexation reaction between Cl^- and SO_4^{2-} with silver ions to generate stable precipitated compounds, which may significantly inhibit the reaction activity of silver, reduce reaction sites on catalyst surface,[35] and ultimately lead to a marked decline in its ability to activate H_2O_2. The coexisting HCO_3^- had little effect on removal process, while NO_3^- had almost no effect on removal reaction.

Natural organic matter (NOM) is another important component of water environment, and the presence of NOM usually has a certain impact on reactions in water, especially on the redox reactions involving reactive oxygen species. As shown in Fig. 5e and f, NOM in water displayed a significant impact on decontamination process of the system. When the NOM concentration was 1 and 3 mg L^{-1}, the bacterial survival density significantly increased from 0 to 1.2 and 2.5 log, and the TC ratio also increased from 0 to 0.18 and 0.43. There may be two reasons for this phenomenon. On the one hand, NOM, as an organic substance, may consume some reactive oxygen species such as $^{\bullet}OH$ in the reaction system, resulting in a decrease in the free radicals used to attack contaminant.[36] On the other hand, NOM may form a complex with silver ions on catalyst surface, which hindered its contact with H_2O_2 and reduced the activation efficiency. While the concentration of NOM is 5 mg L^{-1}, the bacterial density decreased to a certain extent, indicating that NOM played a promoting role at this time. Some reports suggest that NOM can act as an electron donor to bind to catalyst at a certain concentration, thereby promoting catalytic redox reactions through electron transfer. [37]

3.3 Stability evaluation of catalyst

Solution pH is one of the most important factors for catalyst stability in Fenton (like) reaction. Thus, effects of initial pH (5–9) on removal of bacteria and TC were conducted. As depicted in Fig. 6a and b, removal process of bacteria and TC under weakly acidic or neutral conditions presented higher efficiency than that under weakly alkaline conditions. Bacterial inactivation efficiency at pH 5–7 all reached more 5.9 log, which was much higher than 4.5 log at pH 8 and 3.4 log at pH 9. And the removal rate of TC also decreased from 100% at pH 5–7 to 87% at pH 8 and 75% at pH 9. Generally, solution pH value could influence decomposition of H_2O_2 and chemical property of nAg_2O/AC catalyst. It was reported that H_2O_2 is more easily decomposed into $OH^{\bullet}$ under acidic conditions as shown in the following eqn (5).[38] Thus, the generated $OH^{\bullet}$ significantly enhance removal efficiency of bacteria and TC. Conversely, hydroxyl ions (OH^-) in alkaline solution consumed hydrogen ions (H^+) and inhibited the production of $OH^{\bullet}$, eventually leading to a remarkable decrease of removal efficiency. On the other hand, with the continuous increase of pH value, a great quantity of OH^- interacted with Ag(I) in nAg_2O/AC to form stable compounds (see eqn (6) and (7)), [39] consequently reducing the reactivity of this catalyst on activating H_2O_2.[40]

$$M^{n+} + H_2O_2 + H^+ \rightarrow M^{(n+1)+} + {}^{\bullet}OH + H_2O \quad (5)$$

$$Ag(I) + OH^- \rightarrow AgOH \quad (6)$$

$$2AgOH \rightarrow Ag_2O + H_2O \quad (7)$$

Additionally, silver leaching from nAg_2O/AC also was investigated as displayed in Fig. S1.† It showed an ultra-low Ag dissolution rate of nAg_2O/AC below 0.6% at pH 5–9, suggesting its stability within this pH scope. The Ag^+ concentrations in solution between 0.021 to 0.046 mg L^{-1} also met drinking water safety standards (<0.05 mg L^{-1}). In summary, this nAg_2O/AC catalyst successfully broaden the application range of pH to about neutral in Fenton-like reaction, which is very promising in practical water treatment.

To investigate stability of nAg_2O/AC, circular experiment on removal of bacteria and TC was conducted. As observed from Fig. 6c and d, the high inactivation efficiency exceeding 5.2 log could be obtained in the first four cycle tests, and the removal rate of TC could reach over 96% in five cycles tests, indicating the stability of nAg_2O/AC for efficient catalysis of H_2O_2. Based on the previous XRD and SEM results, there was no significant change in the crystal structure and morphology of nAg_2O/AC before and after reaction, and there was only a slight loss of silver content. These characterization results also confirmed the stability of nAg_2O/AC materials. In addition, the extremely low Ag leaching concentration (<0.035 mg L^{-1}) and leaching rate (<0.3%) directly confirmed the stability of catalyst in Fig. S2.† Starting from the fifth cycle, the sterilization effect of the nAg_2O/AC-H_2O_2 system showed a downward trend, which may be attributed to the continuous consumption of highly reactive zero valent Ag in the cyclic reaction (XPS results in Fig. 3 showed a decrease in Ag content and an increase in Ag(I) content after the reaction), resulting in a decrease in the amount of $OH^{\bullet}$ produced by activated H_2O_2. On the other hand, the characteristic peaks of silver in nAg_2O/AC (Fig. 1 and 3) showed no significant changes in intensity in XPS and XRD after the reaction, indicating the stability of the catalyst in cyclic reactions.

After circular experiment, the remaining catalyst solid was cleaned with nitric acid and the obtained activated carbon was used to regenerate catalyst through previous synthesis progress. High removal efficiency of bacteria (5.8 log) and TC (100%) was obtained through the regenerated nAg_2O/AC. This proved the excellent renewability of nAg_2O/AC, implying its potential in practical application.

3.4 Mechanism investigation

The above-mentioned tests and analysis indicated that reactive oxygen species (ROS) generated from nAg_2O/AC heterogeneous Fenton system played an important role in removing bacteria and TC. To identify the contribution of different ROS during

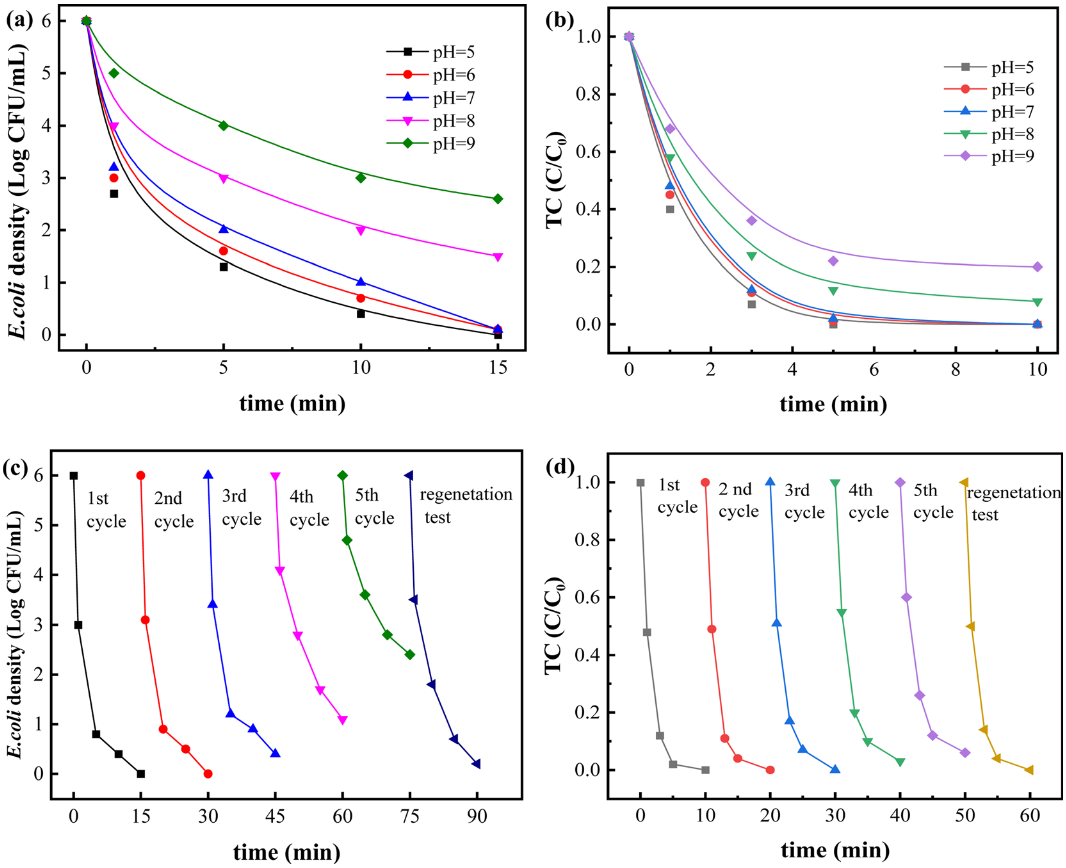

Fig. 6 Effect of initial pH on removal of (a) *E. coli* and (b) TC; (c and d) reusability of nAg_2O/AC in Fenton system. Reaction conditions: 1 g L^{-1} nAg_2O/AC dosage, 4 mM H_2O_2, 10^6 CFU mL^{-1} *E. coli*, 1 mg L^{-1} TC, initial pH 7.0, temperature 30 °C.

reactions, a series of scavenging investigations were carried out with tertbutyl alcohol (TBA), *p*-benzoquinone (BQ) and catalase as the scavenger for $OH^•$, $O_2^{•-}$ and H_2O_2, respectively.[41] As presented in Fig. 7a and b, when no scavenger was involved in nAg_2O/AC heterogeneous Fenton system, the concentration of bacteria and TC decreased rapidly to 0 within 15 min and 10 min, respectively. Similar reaction trends and results could be observed in the presence of BQ and catalase respectively, indicating that effects of $O_2^{•-}$ and H_2O_2 on removal process was minimal or even negligible owing to the low yield of $O_2^{•-}$ and the limited inactivation capacity of H_2O_2.[42] However, after adding TBA into the reaction system, the concentration of bacteria and TC exhibited a significant increase due to the scavenging effect of TBA on $OH^•$ radicals. Bacteria density and TC proportion rose dramatically from 0 to 2.5 log and 0.29 when TBA was 0.5 mM in solution. After adjusting the TBA to 1.0 mM in solution, the bacteria density and TC proportion further increased to 5.2 log and 0.70, and then remained basically unchanged even increasing TBA to 2.0 mM since all $OH^•$ radicals had been scavenged. These results confirmed that the $OH^•$ radicals generated from nAg_2O/AC Fenton system was the major role in removal process and its quantity directly determined the sterilization efficiency.

To directly detect the generated $OH^•$ radicals in reaction, electron spin resonance (ESR) technique was conducted with DMPO as the spin-trapping agents.[27] Fig. 7c displayed that no radical signal was detected in nAg_2O/AC alone system. Slightly different from this, some weak DMPO-$OH^•$ signals appeared in H_2O_2 alone system, implying that a small amount of H_2O_2 could be decomposed into $OH^•$ radicals. However, strong DMPO-$OH^•$ signals characterized by a typical 4-fold peak with an intensity ratio of 1 : 2 : 2 : 1 could be clearly observed in nAg_2O/AC Fenton system. It confirmed that H_2O_2 could be efficiently catalyzed by nAg_2O/AC to produce abundant $OH^•$ radicals. The results were in agreement with the radical scavenging tests (see Fig. 7a and b), in which $OH^•$ radicals were the major ROS in nAg_2O/AC Fenton reaction.

Subsequently, A quantitative analysis towards the amount of $OH^•$ radicals generated from different systems was carried out with fluorescence spectrum. Here, non-fluorescent terephthalic acid (TA) was used to trap $OH^•$ radicals to produce strongly fluorescent hydroxyterephthalic acid (HTA).[27] As depicted in Fig. 7d, the nAg_2O/AC Fenton system exhibited a dramatically enhanced fluorescence signal (435.3) of HTA, which was 6.2 times that of H_2O_2 system (70.5) and 2.9 times that of traditional Fe^{2+} Fenton system (149.6) reported by.[42] To calculate decomposition efficiency of H_2O_2 in different system, total amount of H_2O_2 (represented by total amount of generated HTA) was received by fully heating 100 mL solution containing 32 μL H_2O_2 and 60 mg TA for 60 min. The results demonstrated

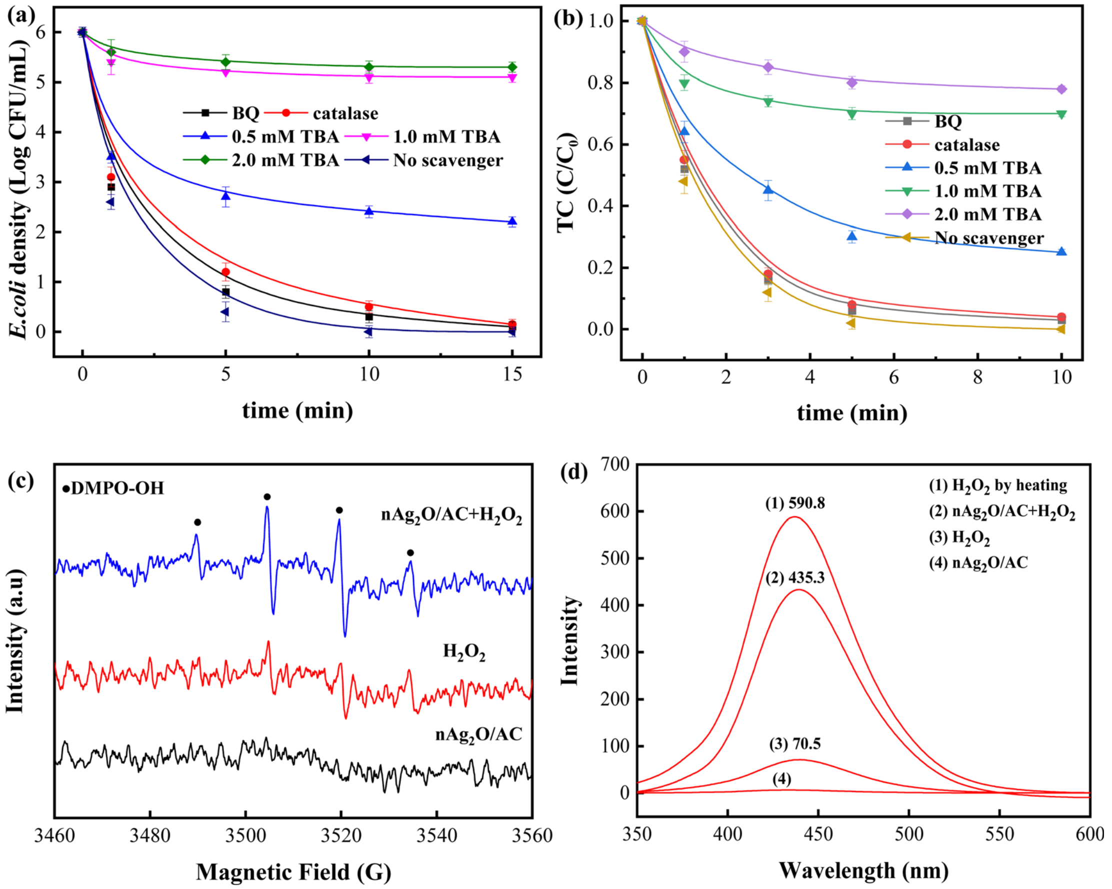

Fig. 7 Effects of various radical scavengers on removal of (a) *E. coli* and (b) TC; (c) ESR spectra for the detection of $OH^{\bullet}$ signal in the presence of 5,5-dimethyl-1-pyrrolidine-*N*-oxide (DMPO), (d) the fluorescence spectrum of terephthalic acid (TA) mixed with different reaction systems after reaction for 5 min. Reaction conditions: 1 g L^{-1} nAg_2O/AC dosage, 4 mM H_2O_2, 10^6 CFU mL^{-1} *E. coli*, 1 mg L^{-1} TC, 1 mM BQ, 1 mM catalase, initial pH 7.0, temperature 30 °C.

that the decomposition efficiency in nAg_2O/AC Fenton system arrived at 73.7% (435.3/590.8 × 100%), which was significantly higher than 11.9% (70.5/590.8 × 100%) in H_2O_2 system and 25.3% (149.6/584.8 × 100%) in traditional Fe^{2+} Fenton system. Hence, it concluded that the nAg_2O/AC could remarkably facilitate the decomposition efficiency of H_2O_2 to produce more $OH^{\bullet}$ in heterogeneous Fenton reaction and $OH^{\bullet}$ is the major ROS accounting for removing bacteria and TC.

Based on the above discussion, a possible reaction mechanism of the nAg_2O/AC Fenton system was proposed as shown in Fig. 8. Firstly, reductive functional groups such as hydroxyl and aldehyde of AC reduced surface-bound Ag(I) in nAg_2O/AC to

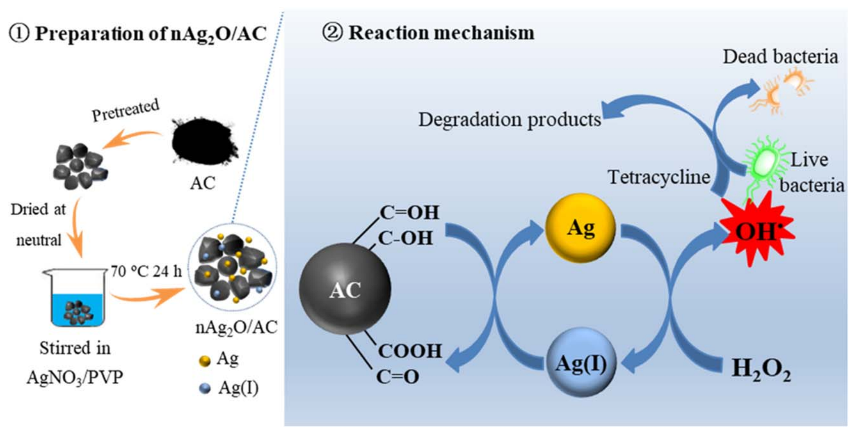

Fig. 8 The proposed reaction mechanism of the nAg_2O/AC Fenton system.

surface-bound Ag by mediated electron transfer process. Then, the generated Ag catalyzed H_2O_2 to produce a great quantity of $OH^•$ radicals. As a strong oxidizing species, the $OH^•$ radicals can effectively degrade micropollutants and inactivate bacteria based on oxidation by attacking cell membranes and proteins, enzymes and genes.[43] Meanwhile, the generated Ag(I) was transformed into Ag again since Ag(I)/Ag cycle was accelerated by the mediated electron transfer of AC. Therefore, the nAg_2O/AC could continuously catalyze H_2O_2 to generate $OH^•$ radicals for enhanced removal of bacteria and micropollutants.

4 Conclusions

In summary, the nAg_2O/AC composite was synthesized as a novel heterogeneous Fenton catalyst and achieved high removal efficiency for *E. coli* and TC in water *via* H_2O_2 activation. Mechanism investigations revealed that reductive functional groups of AC accelerated the Ag(I)/Ag cycle through mediated electron transfer and more Ag catalyzed H_2O_2 to generate abundant $OH^•$ radicals. The $OH^•$ radicals were confirmed to be the major role leading to bacterial inactivation and TC degradation by scavenging tests and ESR analysis. Besides, the effective decomposition rate of H_2O_2 was further quantitatively analyzed by fluorescence spectroscopy. The high removal efficiency at about neutral condition (pH 5–8) in the heterogeneous Fenton reaction made nAg_2O/AC more advantageous in actual water treatment. In addition, the nAg_2O/AC catalyst has good stability and reusability in 5 cycles and regeneration tests, indicating its considerable application prospect. These results demonstrated that nAg_2O/AC as a promising heterogeneous Fenton catalyst is expected to solve the combined contamination problem of bacteria and micropollutants in water. In fact, this work also provides a new perspective for the application of metal oxide as a catalyst for hydrogen peroxide or persulfate in water treatment.

Data availability

The data supporting this article have been included as part of the ESI.†

Author contributions

Jianping Deng: experiment, methodology, software, writing – original draft preparation. Yong Liu: methodology, validation. Shuanglin Gui: validation, project administration. Qizhen Yi: data curation, project administration. Hanbing nie: writing – reviewing and editing, supervision.

Conflicts of interest

The authors declare that they have no known competing financial interests or personal relationships that could have appeared to influence the work reported in this paper.

Acknowledgements

The authors thank the National Natural Science Foundation of China (41977114, 41807338, 52060008).

References

1 X. Y. Ma, Q. Li, X. C. Wang, Y. Wang, D. Wang and N. Huu Hao, Micropollutants removal and health risk reduction in a water reclamation and ecological reuse system, *Water Res.*, 2018, **138**, 272–281.
2 C.-Y. Hu, S.-J. Hua, Y.-L. Lin, Y.-G. Deng, Y.-Z. Hou, Y.-F. Du, C.-D. Dong, C.-W. Chen and C.-H. Wu, Kinetics and formation of disinfection byproducts during iohexol chlor(am) ination, *Sep. Purif. Technol.*, 2020, **243**, 116797.
3 Y. Du, X.-T. Lv, Q.-Y. Wu, D.-Y. Zhang, Y.-T. Zhou, L. Peng and H.-Y. Hu, Formation and control of disinfection byproducts and toxicity during reclaimed water chlorination: A review, *J. Environ. Sci.*, 2017, **58**, 51–63.
4 S. G. Michael, B. Drigo, I. Michael-Kordatou, C. Michael, T. Jaeger, S. C. Aleer, T. Schwartz, E. Donner and D. Fatta-Kassinos, The effect of ultrafiltration process on the fate of antibiotic-related microcontaminants, pathogenic microbes, and toxicity in urban wastewater, *J. Hazard. Mater.*, 2022, **435**, 128943.
5 J. Li, S. Ren, X. Qiu, S. Zhao, R. Wang and Y. Wang, Electroactive Ultrafiltration Membrane for Simultaneous Removal of Antibiotic, Antibiotic Resistant Bacteria, and Antibiotic Resistance Genes from Wastewater Effluent, *Environ. Sci. Technol.*, 2022, **56**(21), 15120–15129.
6 R. Tanveer, A. Yasar, A.-u.-B. Tabinda, A. Ikhlaq, H. Nissar and A.-S. Nizami, Comparison of ozonation, Fenton, and photo-Fenton processes for the treatment of textile dye-bath effluents integrated with electrocoagulation, *Journal of Water Process Engineering*, 2022, **46**, 102547.
7 X. Du, Z. Mo, Z. Li, W. Zhang, Y. Luo, J. Nie, Z. Wang and H. Liang, Boron-doped diamond (BDD) electro-oxidation coupled with nanofiltration for secondary wastewater treatment: Antibiotics degradation and biofouling, *Environ. Int.*, 2021, **146**, 106291.
8 G. Saxena, R. Chandra and R. N. Bharagava, Environmental Pollution, Toxicity Profile and Treatment Approaches for Tannery Wastewater and Its Chemical Pollutants, in *Reviews of Environmental Contamination and Toxicology*, ed. P. de Voogt, Springer International Publishing, Cham, 2017, 240, pp. 31–69.
9 J. T. Jasper, Y. Yang and M. R. Hoffmann, Toxic Byproduct Formation during Electrochemical Treatment of Latrine Wastewater, *Environ. Sci. Technol.*, 2017, **51**(12), 7111–7119.
10 J.-E. Lee, M.-K. Kim, J.-Y. Lee, Y.-M. Lee and K.-D. Zoh, Degradation kinetics and pathway of 1H-benzotriazole during UV/chlorination process, *Chem. Eng. J.*, 2019, **359**, 1502–1508.
11 M. S. Samuel, S. Jose, E. Selvarajan, T. Mathimani and A. Pugazhendhi, Biosynthesized silver nanoparticles using *Bacillus amyloliquefaciens*; Application for cytotoxicity effect

on A549 cell line and photocatalytic degradation of p-nitrophenol, *J. Photochem. Photobiol., B*, 2020, **202**, 111642.
12 X. Kang, D. Teng, S. Wu, Z. Tian, J. Liu, P. Li, Y. Ma and C. Liang, Ultrafine copper nanoparticles anchored on reduced graphene oxide present excellent catalytic performance toward 4-nitrophenol reduction, *J. Colloid Interface Sci.*, 2020, **566**, 265–270.
13 L. Handojo, D. Pramudita, D. Mangindaan and A. Indarto, Application of Nanoparticles in Environmental Cleanup: Production, Potential Risks and Solutions, in *Emerging Eco-Friendly Green Technologies for Wastewater Treatment*, ed. Bharagava, R. N., Springer Singapore, Singapore, 2020, pp. 45–76.
14 H. Su, D. Kow, M. R. Fahmi, C. Z. A. Abidin and O. Soon-An, Advanced Oxidation Processes: Process Mechanisms, Affecting Parameters and Landfill Leachate Treatment, *Water Environ. Res.*, 2016, **88**(11), 2047–2058.
15 B. Song, Z. Zeng, E. Almatrafi, M. Shen, W. Xiong, C. Zhou, W. Wang, G. Zeng and J. Gong, Pyrite-mediated advanced oxidation processes: Applications, mechanisms, and enhancing strategies, *Water Res.*, 2022, **211**, 118048.
16 N. Masomboon, C. Ratanatamskul and M.-C. Lu, Kinetics of 2,6-dimethylaniline oxidation by various Fenton processes, *J. Hazard. Mater.*, 2011, **192**(1), 347–353.
17 A. Babuponnusami and K. Muthukumar, Advanced oxidation of phenol: A comparison between Fenton, electro-Fenton, sono-electro-Fenton and photo-electro-Fenton processes, *Chem. Eng. J.*, 2012, **183**, 1–9.
18 M. Lu, X. Wu and X. Wei, Chemical degradation of polyacrylamide by advanced oxidation processes, *Environ. Technol.*, 2012, **33**(9), 1021–1028.
19 J. Qi, G. Jiang, Y. Wan, J. Liu and F. Pi, Nanomaterials-modulated Fenton reactions: Strategies, chemodynamic therapy and future trends, *Chem. Eng. J.*, 2023, **466**, 142960.
20 C. Zhao, B. Wang, B. K. G. Theng, P. Wu, F. Liu, S. Wang, X. Lee, M. Chen, L. Li and X. Zhang, Formation and mechanisms of nano-metal oxide-biochar composites for pollutants removal: A review, *Sci. Total Environ.*, 2021, **767**, 145305.
21 D. N. Chausov, V. V. Smirnova, D. E. Burmistrov, R. M. Sarimov, A. D. Kurilov, M. E. Astashev, O. V. Uvarov, M. V. Dubinin, V. A. Kozlov, M. V. Vedunova, M. B. Rebezov, A. A. Semenova, A. B. Lisitsyn and S. V. Gudkov, Synthesis of a Novel, Biocompatible and Bacteriostatic Borosiloxane Composition with Silver Oxide Nanoparticles, *Materials*, 2022, **15**(2), 527.
22 J. Deng, B. Li, W. Yin, H. Bu, B. Yang, P. Li, X. Zheng and J. Wu, Enhanced bacterial inactivation by activated carbon modified with nano-sized silver oxides: Performance and mechanism, *J. Environ. Manage.*, 2022, **311**, 114884.
23 G. Su, X. Zhong, S. Qiu, J. Fan, H. Zhou and X. Zhou, Preparation of mesoporous silica-based nanocomposites with synergistically antibacterial performance from nano-metal (oxide) and polydopamine, *Nanotechnology*, 2022, **33**, 155702.
24 B. Li, W. Yin, M. Xu, X. Tan, P. Li, J. Gu, P. Chiang and J. Wu, Facile modification of activated carbon with highly dispersed nano-sized alpha-Fe_2O_3 for enhanced removal of hexavalent chromium from aqueous solutions, *Chemosphere*, 2019, **224**, 220–227.
25 J. Wen, X. Tan, Y. Hu, Q. Guo and X. Hong, Filtration and Electrochemical Disinfection Performance of PAN/PANI/AgNWs-CC Composite Nanofiber Membrane, *Environ. Sci. Technol.*, 2017, **51**(11), 6395–6403.
26 M. Su, Y. Fang, B. Li, W. Yin, J. Gu, H. Liang, P. Li and J. Wu, Enhanced hexavalent chromium removal by activated carbon modified with micro-sized goethite using a facile impregnation method, *Sci. Total Environ.*, 2019, **647**, 47–56.
27 B. Yang, T. Wei, K. Xiao, J. Deng, G. Yu, S. Deng, J. Li, C. Zhu, H. Duan and Q. Zhuo, Effective mineralization of anti-epilepsy drug carbamazepine in aqueous solution by simultaneously electro-generated H_2O_2/O_3 process, *Electrochim. Acta*, 2018, **290**, 203–210.
28 M. Hosseini, A. W. H. Chin, M. D. Williams, S. Behzadinasab, J. O. Falkinham, III, L. L. M. Poon and W. A. Ducker, Transparent Anti-SARS-CoV-2 and Antibacterial Silver Oxide Coatings, *ACS Appl. Mater. Interfaces*, 2022, **14**(7), 8718–8727.
29 Q. L. Shimabuku, T. Ueda-Nakamura, R. Bergamasco and M. R. Fagundes-Klen, Chick-Watson kinetics of virus inactivation with granular activated carbon modified with silver nanoparticles and/or copper oxide, *Process Saf. Environ. Prot.*, 2018, **117**, 33–42.
30 J. S. Choi, H. Lee, Y. K. Park, S. J. Kim, B. J. Kim, K. H. An, B. H. Kim and S. C. Jung, Application of Silver and Silver Oxide Nanoparticles Impregnated on Activated Carbon to the Degradation of Bromate, *J. Nanosci. Nanotechnol.*, 2016, **16**, 4493–4497.
31 N. Chen, H. Xu, X. Jiang, J. Li, Q. Wu, H. Yang and Z. Wu, Ultra-thin silver oxide/silver transparent anodes for high-efficiency organic light-emitting devices, *Appl. Surf. Sci.*, 2022, **603**, 154421.
32 J. Goscianska, I. Nowak, P. Nowicki and R. Pietrzak, The influence of silver on the physicochemical and catalytic properties of activated carbons, *Chem. Eng. J.*, 2012, **189**, 422–430.
33 M. Verma and A. K. Haritash, Degradation of amoxicillin by Fenton and Fenton-integrated hybrid oxidation processes, *J. Environ. Chem. Eng.*, 2019, **7**, 102886.
34 B. Jain, A. K. Singh, H. Kim, E. Lichtfouse and V. K. Sharma, Treatment of organic pollutants by homogeneous and heterogeneous Fenton reaction processes, *Environ. Chem. Lett.*, 2018, **16**, 947–967.
35 C. Lai, X. Shi, L. Li, M. Cheng, X. Liu, S. Liu, B. Li, H. Yi, L. Qin, M. Zhang and N. An, Enhancing iron redox cycling for promoting heterogeneous Fenton performance: A review, *Sci. Total Environ.*, 2021, **775**, 145850.
36 T. Sruthi, R. Gandhimathi, S. T. Ramesh and P. V. Nidheesh, Stabilized Landfill Leachate Treatment using Heterogeneous Fenton and Electro-Fenton Processes, *Chemosphere*, 2018, **210**, 38–43.
37 N. Thomas, D. D. Dionysiou and S. C. Pillai, Heterogeneous Fenton catalysts: A review of recent advances, *J. Hazard. Mater.*, 2020, **404**, 124082.

38 G. Subramanian and H. Prakash, Photo Augmented Copper-based Fenton Disinfection under Visible LED Light and Natural Sunlight Irradiation, *Water Res.*, 2021, **190**, 116719.
39 Y. Zhu, R. Zhu, Y. Xi, J. Zhu, G. Zhu and H. He, Strategies for enhancing the heterogeneous Fenton catalytic reactivity: A review, *Appl. Catal., B*, 2019, **255**, 117739.
40 M. A. Oturan and J.-J. Aaron, Advanced Oxidation Processes in Water/Wastewater Treatment: Principles and Applications. A Review, *Crit. Rev. Environ. Sci. Technol.*, 2014, **44**(23), 2577–2641.
41 W. Li, Z. Wang, H. Liao, X. Liu, L. Zhou, Y. Lan and J. Zhang, Enhanced degradation of 2,4,6-trichlorophenol by activated peroxymonosulfate with sulfur doped copper manganese bimetallic oxides, *Chem. Eng. J.*, 2021, **417**, 128121.
42 J. Liu, C. Dong, Y. Deng, J. Ji, S. Bao, C. Chen, B. Shen, J. Zhang and M. Xing, Molybdenum sulfide Co-catalytic Fenton reaction for rapid and efficient inactivation of Escherichia colis, *Water Res.*, 2018, **145**, 312–320.
43 L. Zarate-Reyes, C. Lopez-Pacheco, A. Nieto-Camacho, E. Palacios, V. Gómez-Vidales, S. Kaufhold, K. Ufer, E. García Zepeda and J. Cervini-Silva, Antibacterial clay against gram-negative antibiotic resistant bacteria, *J. Hazard. Mater.*, 2017, **342**, 625–632.

